Agriculture, Ecosystems and Environment 224 (2016) 104–115

Contents lists available at ScienceDirect

Agriculture, Ecosystems and Environment

journal homepage: www.elsevier.com/locate/agee

How well can we assess impacts of agricultural land management changes on the total greenhouse gas balance (CO_2, CH_4 and N_2O) of tropical rice-cropping systems with a biogeochemical model?

David Kraus[a], Sebastian Weller[a], Steffen Klatt[a], Ignacio Santabárbara[a], Edwin Haas[a], Reiner Wassmann[a,b], Christian Werner[c], Ralf Kiese[a], Klaus Butterbach-Bahl[a,d,*]

[a] Karlsruhe Institute of Technology, Institute of Meteorology and Climate Research (IMK-IFU), Kreuzeckbahnstr. 19, 82467 Garmisch-Partenkirchen, Germany
[b] International Rice Research Institute (IRRI), Los Baños, Philippines
[c] Senckenberg Biodiversity and Climate Research Centre (BiK-F), Senckenberganlage 25, Frankfurt, Germany
[d] International Livestock Research Institute (ILRI), 30709 Naivasha Rd, Nairobi, Kenya

ARTICLE INFO

Article history:
Received 23 September 2015
Received in revised form 10 February 2016
Accepted 24 March 2016
Available online 2 April 2016

Keywords:
LandscapeDNDC
Methane
Nitrous oxide
Soil organic carbon
Rice
Land management change

ABSTRACT

Paddy rice is the main cropping system in Southeast Asia. However, water scarcity arising from competition from other sectors, rainfall variability and climate change increasingly challenges global rice production. One option to adapt to lower water availability is switching from paddy rice to less irrigation intensive upland cropping systems. Such land management change (LMC) is likely to significantly affect ecosystem carbon and nitrogen cycling and its greenhouse gas (GHG) balance. This study evaluates how well the ecosystem model LandscapeDNDC is able to simulate observed emissions of methane (CH_4), nitrous oxide (N_2O) and carbon dioxide (CO_2) from different tropical cropping rotations, i.e., double- and triple-cropped paddy rice, aerobic rice–paddy rice and maize–paddy rice (rice: *O. sativa*, maize: *Zea mays*) and how management changes to rice dominated lowland systems will affect the GHG balance on short (a few years) and long (several decades) time scales.

LandscapeDNDC predicts seasonal emissions of CH_4 and N_2O across different cropping rotations (including LMC) with R^2 values of 0.85 and 0.78 and average underestimations of 15 and 14%, respectively. In addition to emissions of CH_4 and N_2O, LandscapeDNDC also captures the long-term development of soil organic carbon (SOC). Soil oxygen status, growth of photosynthetic active aquatic biomass as well as decomposability of harvest residues significantly influence SOC development.

Simulation results demonstrate that short-term GHG balances after LMC considerably differ from long-term balances. Simulated total GHG emissions three years after LMC are highest for upland crop – paddy rice rotations due to pronounced decomposition of soil organic carbon. In contrast, the total GHG emissions are highest for double cropping of paddy rice and are clearly dominated by CH_4 emissions over a longer period of several decades. Simulation results suggest that approx. 2.8–3.4 t C ha^{-1} yr^{-1} residue incorporation after harvest is needed to achieve stable SOC stocks in mixed upland crop–paddy rice systems after LMC from double-cropped paddy rice systems.

1. Introduction

Carbon dioxide (CO_2), methane (CH_4) and nitrous oxide (N_2O) contribute approximately 80% to the current global radiative forcing of well-mixed greenhouse gases (GHG) (Myhre et al., 2013). Among the most important anthropogenic emission sources of these GHG are emissions from land use and land management change (Ciais et al., 2013). Whereas flooded rice represents a major source of atmospheric CH_4, effectively all cropping systems are major emitters of N_2O, mainly due to the use of synthetic fertilizer for increasing crop production. However, the actual amount of N_2O emission varies depending on fertilization intensity, cropping system and other factors. Global source estimates in the year 2005 for these two atmospheric gases are 25–30 Tg CH_4-C yr^{-1} and 1.7–4.4 Tg N_2O-N yr^{-1}, representing approx. 1.5 and 5% of total anthropogenic GHG emissions, respectively (Herzog, 2009). After

* Corresponding author at: Karlsruhe Institute of Technology, Institute of Meteorology and Climate Research (IMK–IFU), Kreuzeckbahnstr. 19, 82467 Garmisch-Partenkirchen, Germany.
E-mail address: klaus.butterbach-bahl@kit.edu (K. Butterbach-Bahl).

http://dx.doi.org/10.1016/j.agee.2016.03.037
0167-8809/

fossil fuel combustion, land use change (LUC) is the second most important source of anthropogenic CO_2 emissions. LUC has led to the release of approx. 180 Pg CO_2-C to the atmosphere since 1750 (Ciais et al., 2013) and is responsible for approx. 12% of total anthropogenic GHG emissions (reference year 2005; Herzog, 2009). Although at present the transformation of (sub-) tropical forests into agricultural systems and the related loss of plant biomass as well as soil organic carbon (SOC) is responsible for the largest part of LUC related CO_2 emissions (Don et al., 2011; Ciais et al., 2013), land management changes (LMC) such as the conversion of lowland (e.g., rice paddy production systems) into upland (e.g., maize) agricultural systems may result in large additional loss of SOC (Witt et al., 2000).

Paddy rice provides stable food to 1/3 of the world population (Devendra and Thomas, 2002) and is the dominating cropping system in Southeast Asia. Increasing water scarcity, changes in diets and demands from other sectors, e.g., biofuel production, however, leads to a growing number of farmers diversifying paddy rice with upland crop cultivation (Timsina et al., 2010, 2011). This is likely to cause major changes in the emissions of GHG from such systems. Weller et al. (2015b) recently reported that the change from paddy rice cultivation to upland maize production leads to "pollution swapping" with average seasonal CH_4 emissions decreasing from 58 ± 21 kg CH_4-C ha^{-1} to close to zero, while N_2O emissions substantially increase from 0.6 ± 0.3 to 3.9 ± 0.8 kg N_2O-N ha^{-1} under conventional fertilizer practices. However, consequences of such land management changes on SOC stocks remain still unclear.

In recent decades, numerous studies have been published on CH_4 and N_2O emissions from tropical cropping systems (e.g., Babu et al., 2006; Linquist et al., 2012; Wassmann et al., 2004; Weller et al., 2015a,b). Likewise, many studies analyze SOC dynamics in tropical lowland systems (e.g., Olk et al., 1996; Pampolino et al., 2008) as well as mixed lowland – upland systems (e.g., Huang et al., 2012; Pan et al., 2003; Wu, 2011; Yadav et al., 1998). So far only few studies (Cheng et al., 2014; Li et al., 2005; Shang et al., 2011) simultaneously evaluate N_2O, CH_4 and SOC stock changes and their contributions to the total GHG balance of an agricultural system or distinguish between short-term and long-term effects (Frolking et al., 2004; Li et al., 2005). The latter point is of primary importance since impacts of SOC decomposition on the GHG flux balance, in contrast to emissions of CH_4 and N_2O, is limited in the long-term by the establishment of a new equilibrium. Depending on the C input and outflow of the system, this equilibrium will occur most likely at a lower level (Johnston et al., 2009). Based on emission data from a recent field experiment (Weller et al., 2015a, 2016) at the International Rice Research Institute (IRRI), Philippines, our study contrasts short-term (3 years) and long-term (>30 years) impacts of land management changes on the total GHG balances (CH_4, N_2O and CO_2) of paddy rice cropping systems with the biogeochemical model LandscapeDNDC (Haas et al., 2013; Kraus et al., 2015). While it was shown that the $MeTr^x$ (Metabolism and Transport of compound x) biogeochemical submodel of LandscapeDNDC is able to simulate CH_4 and N_2O emissions from tropical lowland and upland systems (Kraus et al., 2015), the predictability of SOC dynamics on longer time scales has so far not been evaluated. Therefore, we tested the model on available datasets of long-term SOC changes of tropical rice-based cropping systems before applying it for simulating scenarios.

2. Material and methods

2.1. Field experiments

In this study, we examine three different field experiments that are conducted at the Experimental Station of the International Rice Research Institute (IRRI), Los Baños, Philippines (14°09′45″ N, 121°15′35″ E, 21 m a.s.l.), i.e., the long-term continuous cropping experiment (LTCCE), the long-term fertility experiment (LTFE) and the ICON experiment (Introducing Non-Flooded Crops in Rice-Dominated Landscapes: Impacts on Carbon, Nitrogen and Water Cycles). The Investigated crop rotations include paddy rice (*O. sativa*) and maize (*Z. mays*). While the LTCCE and the LTFE experiment have been started in the 1960s, the ICON experiment has been initiated only recently in 2012.

2.1.1. LTCCE experiment

The long-term continuous cropping experiment (LTCCE) at IRRI investigates the sustainability of intensive triple-cropped paddy rice cultivation under four different urea fertilizer regimes, i.e., no fertilizer, 120, 240 and 360 kg N ha^{-1} yr^{-1} (LTCCE0, LTCCE120, LTCCE240, LTCCE360) (Pampolino et al., 2008). The experiment started in 1963 with originally two rice crops per year and was intensified to three rice crops per year from 1966 onwards (one crop in the dry season [DS] and two crops in the early and late wet season [WS]). In the years 1991, 1993 and 1994 only two rice crops were cultivated with either dry or wet fallow periods in between growing seasons (Dobermann et al., 2000). Aboveground crop residues are completely removed after harvest (no stubbles left on the field). After soil puddling the soil is kept at saturated hydraulic conditions (no standing water) until 14 days after transplanting. Subsequently a water table of 0.05–0.1 m is maintained until harvest.

2.1.2. LTFE experiment

The long-term fertility experiment (LTFE) at IRRI compares the effect of different fertilizer regimes on yields for double-cropped paddy rice systems. The fertilizer regimes differ with respect to the amount of added nitrogen, phosphorus and potassium. Since LandscapeDNDC does not consider the latter two, only the amount of nitrogen is accounted for, which varies in the experiments between 0 and 250 kg N ha^{-1} yr^{-1} (LTFE0, LTFE250). After harvest, approx. 60% of straw yield is incorporated into the soil.

2.1.3. ICON experiment

The ICON experiment aims to explore environmental consequences of the change in management from double-cropped paddy rice cultivation to paddy rice (WS) diversified with upland crops in the DS, a management practice that is increasingly applied across Southeast Asia (Häfele et al., 2013; Timsina et al., 2011). The experiment encompasses three different cropping rotations, i.e., paddy rice–paddy rice (R), aerobic rice–paddy rice (A) and maize–paddy rice (M) (paddy rice: Tubigan 18, aerobic rice: Sahod Ulan 1, maize: Pioneer hybrid 30T80). Prior to the start of the experiment in the DS 2012, all fields were cropped with paddy rice in the DS and WS for at least two decades. For all cropping rotations three different fertilizer regimes are applied, i.e., no fertilizer, conventional fertilizer and optimized site-specific fertilizer application (0–180 kg N ha^{-1} $season^{-1}$, see Weller et al., 2016). The experimental data so far covers five consecutive cropping seasons from the DS 2012 to the DS 2014.

2.2. Model description

LandscapeDNDC is a simulation framework (Grote et al., 2009; Haas et al., 2013), which allows combination of various submodels describing water, carbon and nitrogen cycling and exchange processes with the atmosphere and hydrosphere of forest (Dirnböck et al., 2016; Molina-Herrera et al., 2015), grassland (Wolf et al., 2012; Molina-Herrera et al., 2016) and cropland ecosystems (Chirinda et al., 2011; Kim et al., 2014, 2015; Molina-Herrera et al., 2016). Kraus et al. (2015) extended

LandscapeDNDCby the biogeochemical submodel MeTr^x, which describes plant and soil organic matter by distinctive carbon and nitrogen pools. Plant litter is classified by measurable contents of lignin, cellulose and solutes, whereas soil organic matter is characterized by the degree of humification, i.e., young, old and very old humus. All pools are subject to decomposition and humification depending on pool-specific rate constants, environmental factors (e.g., temperature, moisture and pH) as well as pool quality related factors (e.g., lignin concentration and C/N ratio). Moreover, decomposition rates are reduced under a naerobic conditions. Decomposition of plant and soil organic matter drives the microbial mediated processes ammonification, nitrification, denitrification, fermentation, and methane-production/-consumption. Aerobic conditions promote nitrification, methane and iron oxidation, while anaerobic conditions support denitrification, fermentation, iron-reduction and methane-production (Kraus et al., 2015). Respective aerobic and anaerobic parts of the soil are determined by corresponding soil oxygen concentrations. A specific feature of flooded ecosystems such as paddy rice fields is the growth of photosynthetic active aquatic biomass (PAB) (Roger, 1996). MeTr^x includes a simple routine that derives growth of PAB from incoming solar radiation at the water surface level. The biogeochemical MeTr^x submodel is run in combination with four additional submodels that simulate canopy microclimate, soil-temperature, soil-hydrology and plant growth. All submodels run consecutively using an hourly simulation time step and a vertical soil layer resolution of 0.02 m.

2.3. Model improvements

All considered field experiments distinguish different fertilizer rates. Nitrogen fertilizer in paddy rice fields can exert both stimulating as well as suppressing effects on CH_4 emissions (Bodelier and Laanbroek, 2004; Banger et al., 2012). The most obvious stimulating effect of nitrogen on CH_4 emissions is the increase of gross primary production promoting higher carbon and thus methanogenic substrate availability (Aulakh et al., 2001). On the other hand, nitrogen can increase methanotrophic activity leading to lower CH_4 emissions (Bodelier and Laanbroek, 2004). We added two new nitrogen response factors in the former formulations of gross primary production of photosynthetic active aquatic biomass (PAB) as well as methane oxidation. The growth rate of PAB (r_{PAB}) is now given by

$$r_{PAB} = \left[(1 - f_{N,1})k_{PAB} + f_{N,1}f_{N,2}k_{PAB}\right]r_{pa},$$

wherein $f_{N,1}$ is a weighting factor for the influence of nitrogen on r_{PAB}, $f_{N,2}$ is a Michaelis-Menten response factor with respect to nitrogen availability (amount of ammonia [NH_3], ammonium [NH_4^+] and nitrate [NO_3^-] dissolved in the surface water), r_{pa} is the photosynthetic active shortwave radiation that reaches the surface water after passing the canopy and k_{PAB} is an empirical rate constant for the growth of PAB.

Methane oxidation ($r_{CH_4,ox}$) is given by

$$r_{CH_4,ox} = \mu_{CH_4,ox} f_{CH_4} f_{O_2} f_N f_T,$$

wherein f_T is a response factor for temperature and f_{CH_4}, f_{O_2} and f_N are Michaelis-Menten response factors for CH_4, O_2 and nitrogen availability, respectively.

2.4. Model input description

Model drivers for all LandscapeDNDC model setups include air chemistry, weather, soil-texture and agricultural management information.

2.4.1. Air chemistry

Air chemistry input involves daily information of nitrogen deposition (NH_4^+ and NO_3^- either as wet or dry deposition) as well as atmospheric concentrations of CO_2. In this study, atmospheric concentration of CO_2 corresponds to historic observations until the year 2015 (401 ppbv) and is kept constant on the level of 2015 afterwards (i.e., no air chemistry scenario is used). Input information for atmospheric nitrogen deposition is given as NH_4^+ and NO_3^- concentrations in precipitation and kept constant throughout the complete simulation period ($C_{NH_4^+} = C_{NO_3^-} = 0.3\ mg\ l^{-3}$). Note that in our simulations atmospheric nitrogen deposition is coupled to days with rainfall (Li et al., 2000).

2.4.2. Weather data

The regional climate encompasses two characteristic seasons, i.e., the dry season (DS) lasting from January to May and the wet season (WS) lasting from June to December with average (1978–2014) amounts of rainfall of 300 mm and 1706 mm, respectively. For the same period the annual mean, maximum and minimum temperatures are 27.1, 30.7 and 23.5 °C, respectively (IRRI Climate Unit). For the simulation periods 1958–1978 as well as 2014–2100 daily weather information is replicated from the dataset 1978–2014, i.e., no climate change scenario is considered.

2.4.3. Soil properties

Reported soil properties and changes in SOC predominantly refer to the puddled topsoil horizon expanding to 0.2 m soil depth (Pampolino et al., 2008). Nevertheless, simulated soil depth is constantly set to 0.6 m throughout all simulations in order to provide suitable conditions for numerical calculations of soil hydrology and soil temperatures. All information on topsoil texture is taken from Cassman et al. (1995), Pampolino et al. (2008) and Weller et al. (2015a, 2016). Mass balances of topsoil SOC stocks rely on measurements of bulk density (Table 1) and SOC concentration (Table 2). Unfortunately, there are only bulk density measurements available for the years 1998 (LTCCE), 2000 (LTFE) and 2014 (ICON), with topsoil bulk density being known to vary with field management such as ploughing. In contrast, measurements of

Table 1
Soil-texture properties of the 0–0.2 m soil horizon for the LTCCE, LTFE and ICON experimental sites. For each experiment, the soil is classified as 'Andaqueptic Haplaquoll' (USDA classification).

	Bulk density [g cm^{-3}]	pH [-]	Fe [μ mol g^{-1}]	Sand [%]	Silt [%]	Clay [%]	Wilting point [%]	Field capacity [%]
LTCCE	0.69	6.1	273.4	6.0	30.0	64.0	57.0	42.0
LTFE	0.65	5.9	273.4	10.0	35.0	55.0	55.0	37.0
ICON	1.0 ± 0.05	6.3	273.4	13.0	33.0	54.0	50.0	36.0

Bulk density, pH, sand, silt and clay content are taken from Pampolino et al. (2008) and Weller et al. (2015a, 2016). Iron content (Fe) is assumed to equal Maahas soil at IRRI (Yao et al., 1999). Wilting point and field capacity are derived by pedotransfer function and presented as a percentage with respect to total soil volume. All data from LTCCE and LTFE originate from the years 1998 and 2000.

Table 2
Topsoil (0–20 cm) organic carbon concentrations (%) for the LTCCE, LTFE and ICON experimental sites. All data taken from Cassman et al. (1995),Pampolino et al. (2008) and Weller et al. (2016).

	LTCCE 0[a]	LTCCE 120[a]	LTCCE 240[a]	LTCCE 360[a]	LTFE 0[a]	LTFE 250[a]	ICON R[b]	ICON A[b]	ICON M[b]
1963	1.83[c]	1.83[c]	1.83[c]	1.83[c]	–	–	–	–	–
1964	–	–	–	–	2.00[c]	2.00[c]	–	–	–
1982	–	–	–	–	1.89	2.04	–	–	–
1983	2.20	2.22	2.35	2.49	–	–	–	–	–
1984	–	–	–	–	2.13	2.40	–	–	–
1988	–	–	–	–	1.93	2.12	–	–	–
1991	2.27	2.31	2.43	2.62	1.82	1.99	–	–	–
1998	2.35	2.45	2.55	2.66	–	–	–	–	–
2000	–	–	–	–	2.26	2.26	–	–	–
2011	–	–	–	–	–	–	1.58 ± 0.25	1.58 ± 0.25	1.58 ± 0.25
2014	–	–	–	–	–	–	1.66 ± 0.23	1.62 ± 0.22	1.49 ± 0.19

[a] Refers to treatment specific nitrogen fertilizer load (kg N ha^{-1} yr^{-1}).
[b] Cropping rotation (R: paddy rice–paddy rice; A: aerobic rice–paddy rice; M: maize–paddy rice).
[c] Refers to composite sample (Cassman et al., 1995).

SOC concentrations are available for the initial state as well as for several points of time over the course of the experiments. As a consequence, all SOC stocks in our study are derived under the assumption of constant bulk density, i.e., measured bulk densities at the end of the considered experimental time span are assumed to having prevailed over the entire experiment. Additional soil texture information for all experiments is provided in Table 1. All soil layers below topsoil (soil depth > 0.2 m) are assumed to contain substantially less SOC and are set to 0.5% by default.

2.4.4. Management

LandscapeDNDC offers numerous management options, e.g., planting/harvesting of crops, fertilizing, puddling/ploughing, irrigation and flooding. Information about the respective management options for the different rotations of the ICON experiment can be found in Kraus et al. (2015) and Weller et al. (2015a, 2015b, 2016). Management settings for the LTCCE and LTFE are obtained from Cassman et al. (1995), Dobermann et al. (2000) and Pampolino et al. (2008).

Planting/Harvesting: In the ICON experiment, all planting and harvesting dates correspond to actual dates (Weller et al., 2016). After harvest a constant stubble height of 0.1 m for all rice plants is implemented, whereas for maize all aboveground biomass is removed (no stubbles left on the field). For the LTCCE as well as for the LTFE we use a uniform set of management practices for all years according to the literature.

In the LTCCE, all three cropping and fallow periods are equally sized. After harvest all aboveground biomass is removed from the field (no stubbles left on the field). In the LTFE, we establish two equally sized cropping periods per year, one in the DS (here: February, 1–May, 10) and one in the WS (July, 1–September 18). After harvest a constant stubble height of 0.1 m (LTFE0) and 0.2 m (LTFE250) is implemented corresponding to reported annual carbon inputs from aboveground biomass of 1.5 and 2.0 t C ha^{-1} yr^{-1} in the LTFE0 and LTFE250, respectively (Pampolino et al., 2008).

Fertilizing: In all experiments (ICON, LTCCE and LTFE), urea is exclusively used as fertilizer. Fertilizer application in the ICON experiment is split into three applications with dates and amounts corresponding to reported values. Fertilizer is applied at 0.05–0.1 m soil depth in the maize season and applied at the surface in the rice seasons. In the LTCCE and LTFE, fertilizer application is split into two events with two-thirds being applied at transplanting and one-third 30 days later. As in the ICON experiment for paddy rice cultivation, urea is applied at the soil surface.

Land preparation: Land preparation in paddy rice systems typically includes ploughing following harvest and various harrowing events (breakup of soil aggregates) within a time period of approx. 3–4 weeks. In all experiments of this study, field preparation is implemented in form of two ploughing/harrowing events (till depth: 0.2 m). The time intervals between the ploughing events are set to 10 days in the LTCCE (due to short fallow period) and 20 days in the LTFE. For the ICON experiment actual dates are used. According to Dobermann et al. (2000) who report that fields of the LTCCE do rarely dry out during 15–20 days fallow periods, we implement 17 days long fallow periods with the soil set water saturated below 0.05 m soil depth and kept at field capacity in the upper 0.05 m.

Flooding: In the LTCCE and LTFE the soil is kept flooded from two weeks after transplanting until harvest. For the ICON experiment the actual recorded dates are used. Soil puddling, i.e., field ploughing under water-saturated conditions leads to the formation of a dense plough pan that effectively reduces water percolation during the flooded cropping season (Kögel-Knabner et al., 2010). Between ploughing and field drainage the water percolation rate in all rice fields (including aerobic rice) is capped at a maximum value of 3.0 mm per day, which is a typical value reported for clay-dominated soils after soil puddling (Bouman and Tuong, 2001; Bouman et al., 2007).

2.5. Uncertainty analysis

We perform several uncertainty analyses with respect to the SOC stock development in the LTCCE and the LTFE. For the LTCCE, we investigate (a) the influence of the growth of photosynthetic active aquatic biomass (PAB) by changing the growth rate constant k_{PAB} and (b) the influence of the hydrologic conditions during the fallow period by changing the assumed depth of the groundwater table. For the LTFE we investigate (a) the influence of shorter time periods of soil submergence, i.e., early field drainage two weeks before harvest and (b) the influence of increased decomposition of aboveground biomass. All sensitivity analyses extend till the year 2100 in order to investigate the SOC stock development beyond the experimental time frames.

2.6. Calculation of total GHG balance

The GHG balance in this study includes net ecosystems fluxes of N_2O, CH_4 and CO_2. For this balance CO_2 fluxes are calculated as the net ecosystem exchange (NEE, negative values indicate CO_2

uptake) plus harvest removals. The total GHG balance of the soil is expressed in CO_2-equivalents using the reported values of specific global warming potentials according to the 2007 IPCC report (Denman et al., 2007), i.e., 298 and 25 for N_2O and CH_4, respectively:

$$\text{GHG } (CO_{2eq}\ \text{Mg ha}^{-1}) = (\text{NEE} + \text{harvest\_C})\ (\text{Mg } CO_2\ \text{ha}^{-1}) + 25\ CH_4\ (\text{Mg } CH_4\ \text{ha}^{-1}) + 298\ N_2O\ (\text{Mg } N_2O\ \text{ha}^{-1})$$

Note that this GHG balance neither includes lifecycle assessment of harvested and removed aboveground biomass nor considers the indirect global warming potential of oxidized methane (Boucher et al., 2009).

2.7. Statistical evaluations

The coefficient of determination (R^2), Nash-Sutcliffe efficiency (NSE) and root mean square prediction error (RMSPE) are used to assess quality of agreement of model simulation (x) and field measurements (y):

$$R^2 = \frac{(\Sigma(x-\overline{x})\Sigma(y-\overline{y}))}{\Sigma(x-\overline{x})^2\Sigma(y-\overline{y})^2 (0 \le r^2 \le 1)}$$

$$NSE = 1 - \frac{\Sigma(x-y)^2}{\Sigma(y-\overline{y})^2 (-\infty \le NSE \le 1)}$$

$$RMSPE = \frac{\sqrt{\Sigma(x-y)^2}}{n}$$

3. Results

3.1. Aboveground biomass production

Temporal development of simulated aboveground biomass (AGB) of the mixed-maize, mixed-rice and paddy rice rotation in the ICON experiment is generally within the uncertainties of observations (Fig. 1). Since site-specific optimized fertilization in the field or implemented in model runs did not cause significant differences in AGB (data not shown), we only present results of the conventional and unfertilized treatments. Largest deviations for the conventional fertilized treatment occur in the wet season (WS) 2013 in which AGB is underestimated by 18–26%. For the unfertilized treatment (ICON experiment) AGB of observations and simulations is on average about 50% and 40% lower, respectively. Largest overestimations of simulated AGB in the unfertilized treatments occur in the dry season (DS) 2012 in the paddy rice rotation (59%) and in the WS 2012 in the mixed-maize rotation (65%).

For the LTCCE and LTFE we do not show simulation results of AGB for single seasons due to missing observational data and lack of management information on planting and harvesting or fertilizer application. Observed yields for the LTCCE0 and LTCCE360 vary greatly during the experimental time period with reported averages of 5.8 and 3.9 t DW ha^{-1}, respectively (Dobermann et al., 2000). The average simulated yield for the LTCCE360 in our study is 6.4 t DW ha^{-1} (overestimating observations by approx. 10%). For the LTCCE0 simulated average yield is 3.6 t DW ha^{-1} (underestimating observed yields by 8%).

3.2. SOC dynamics

3.2.1. LTCCE and LTFE

Fig. 2 (top) illustrates simulated and measured topsoil SOC dynamics for the different fertilizer treatments of the LTCCE and the LTFE. Simulated SOC dynamics from both experiments show a clear response to differences in land management changes since the 1960s.

In the LTCCE, simulated SOC stocks of all fertilizer treatments increase continuously over time, except for the period 1991–1995. In these years rice production was changed from three to two cultivated crops per year, which resulted in short-term SOC stock reductions. All fertilizer treatments (0–360 kg N ha^{-1} yr^{-1}) of triple-cropped paddy rice lead to stronger increase of SOC stocks compared to the control treatment with double-cropped paddy rice (annual fertilization rate: 200 kg N ha^{-1} yr^{-1}). Increasing fertilizer amounts enhances simulated SOC stock accumulation ranging from 195 kg C ha^{-1} yr^{-1} (LTCCE0) to 321 kg C ha^{-1} yr^{-1} (LTCCE360). The dependency of simulated SOC stock accumulation on different N fertilization rates is in good agreement with observed patterns. Within the considered time frame of the experiment (1963–1998), the observed cumulative amounts of sequestered carbon are 6.8 and 11.2 t C ha^{-1} in the LTCCE0 and LTCCE360, respectively. The simulated SOC stocks in the year 1998 deviate from observations by less than 5%.

In contrast to the LTCCE, LTFE observations of SOC stocks do not increase but rather fluctuate between individual measurement years and simulations do not reproduce these patterns. In the year

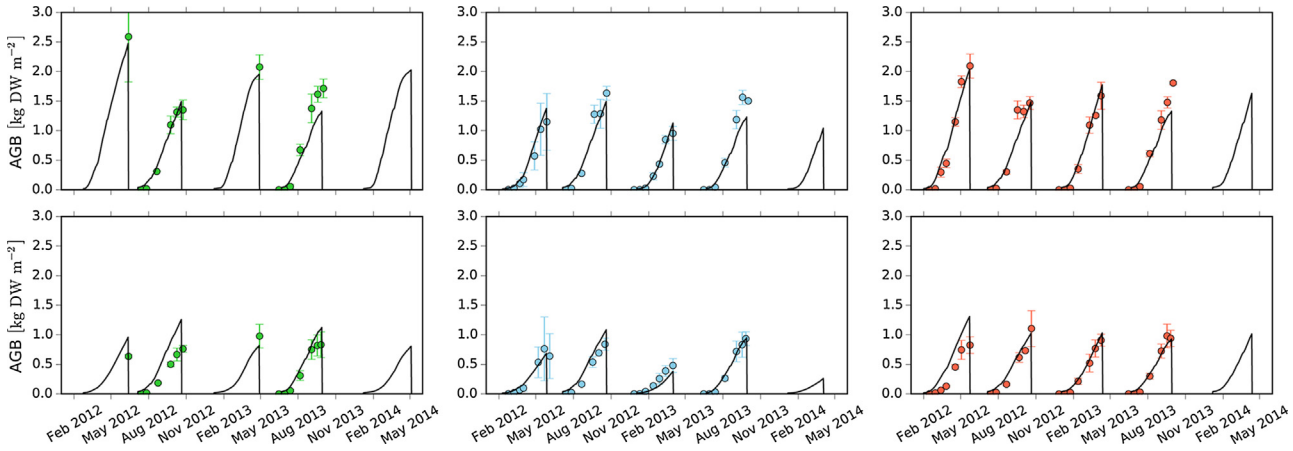

Fig. 1. Daily simulated and observed aboveground biomass (AGB) development for different fertilizer treatments (conventional: upper row; unfertilized: lower row) and crop rotations (mixed-maize: green, left; mixed-rice: blue, center; paddy rice: red, right) in the ICON experiment. Error bars represent the standard deviation of the observations (n = 3). (For interpretation of the references to colour in this figure legend, the reader is referred to the web version of this article.)

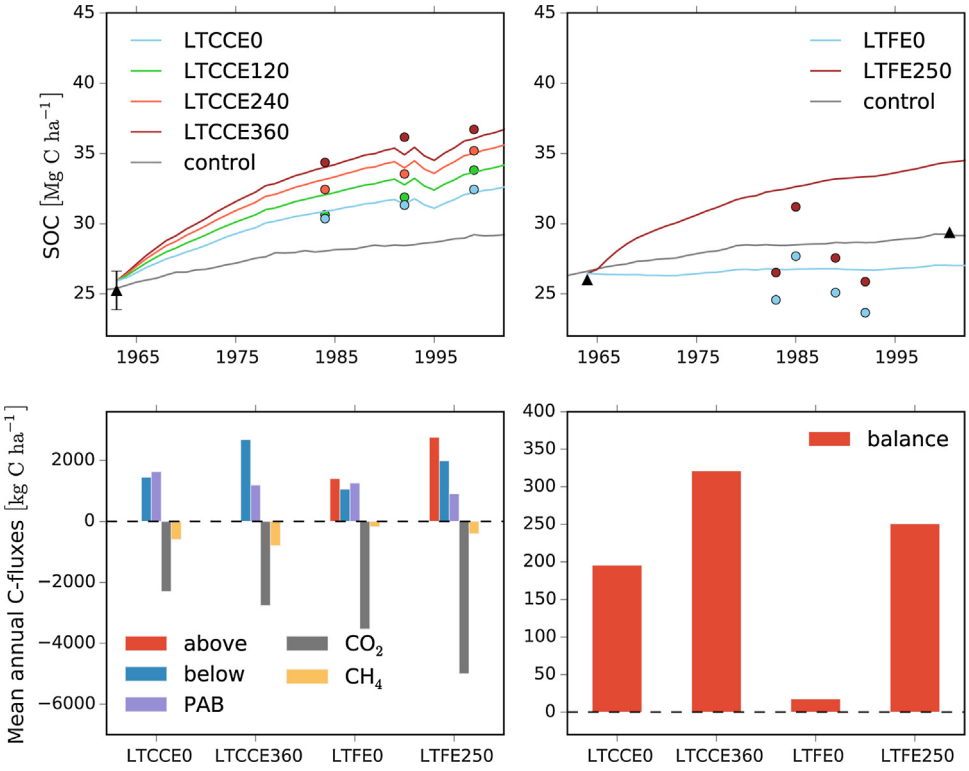

Fig. 2. (top) Dynamics of simulated and observed topsoil (0–0.2 m) SOC stocks for the LTCCE (left) and the LTFE (right). Control runs continue the assumed pre-experimental management of double-cropped paddy rice cultivation. Black triangle symbols refer to mixed samples across fertilizer treatments. Bottom left: annual means of simulated ecosystem C fluxes for the different fertilizer treatments of the LTCCE and the LTFE. Carbon fluxes represent simulated SOC input via below- and aboveground plant litter and photosynthetic active aquatic biomass (PAB) as well as losses via emissions of CH_4 and CO_2. Bottom right: balances of the respective simulated ecosystem C fluxes.

2000, simulated SOC stocks of LTFE0 and LTFE250 are on average 7% below and 15% above the measured mean value. Compared to the LTCCE, the LTFE treatments show lower increases of the SOC stock with time. In the LTFE0 and LTFE250, the mean rates of SOC stock changes for the topsoil are 18 and 251 kg C ha^{-1} yr^{-1}.

In addition to SOC accumulation, Fig. 2 (bottom) also shows simulation results of major ecosystem carbon fluxes for the LTCCE and LTFE experiments, i.e., carbon inputs via below- and aboveground plant biomass and photosynthetic active aquatic biomass (PAB) as well as carbon losses due to heterotrophic respiration and CH_4 emissions. In both experiments, simulated growth of PAB is approx. 40% larger in the treatments without fertilizer application (LTCCE0/360: 1.6/1.2 t C ha^{-1} yr^{-1}, LTFE0/250: 1.3/0.9 t C ha^{-1} yr^{-1}). In contrast to PAB, carbon inputs via below- and aboveground plant litter is 85 and 93% higher in the LTCCE360 (2.7 t C ha^{-1} yr^{-1}) and LTFE250 (4.7 t C ha^{-1} yr^{-1}) as compared to respective treatments without fertilizer application (LTCCE0: 1.5 t C ha^{-1} yr^{-1}, LTFE0: 2.5 t C ha^{-1} yr^{-1}). Although total carbon input on average (mean over all fertilizer treatments) is 35% higher in the LTFE as compared to the LTCCE, 41% higher carbon losses due to soil respiration and CH_4 emissions lead on average to 90% higher SOC stock accumulation in the LTCCE as compared to the LTFE.

Fig. 3 (left) illustrates the sensitivity of SOC stocks in the LTCCE0 and LTCCE360 with regard to a) the growth rate of PAB and b) soil hydrological conditions. The complete suppression of PAB leads to 42 (LTCCE0) and 18% (LTCCE360) lower SOC stocks (reference year: 2100) as compared to the default setting, while doubling the growth rate constant of PAB leads to 37 (LTCCE0) and 20% (LTCCE360) higher SOC stocks in the topsoil. Increasing saturated conditions in the fallow period from 0.05 m soil depth to the soil surface results in 16 (LTCCE0) and 22% (LTCCE360) higher SOC stocks. With the exception of the control run and the

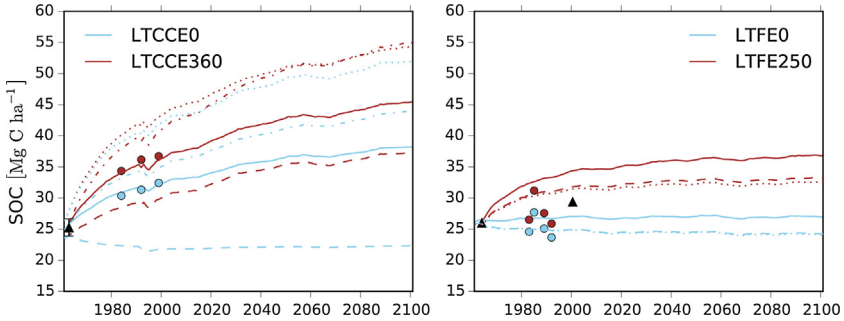

Fig. 3. (left) Sensitivity analyses of changed growth rates of photosynthetic active aquatic biomass (PAB) (increased growth of PAB: dotted, no growth of PAB: dashed) and hydrologic conditions during post-harvesting periods (dash-dotted) on topsoil (0–0.2 m) SOC dynamics for the LTCCE0 and LTCCE360. Right: Sensitivity analyses of topsoil SOC stock dynamics in the LTFE regarding increased decomposability of aboveground biomass (dotted) and reduced time period of field flooding (dashed). The solid lines in the LTCCE (left) and LTFE (right) continue unchanged experimental conditions.

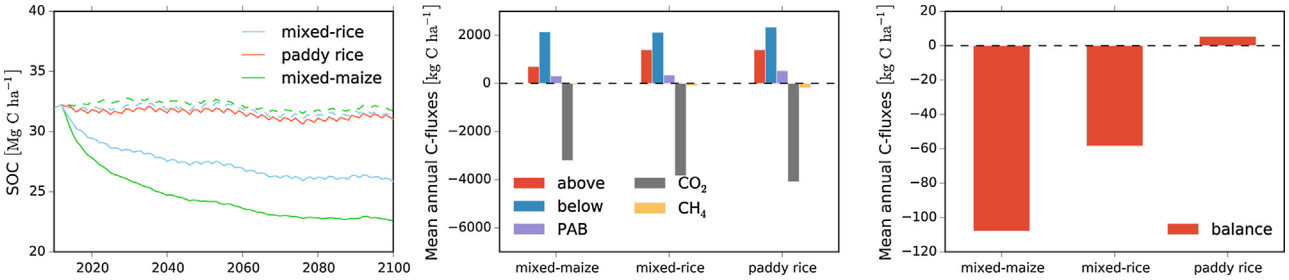

Fig. 4. (left) Simulated topsoil (0–0.2 m) SOC stock dynamics for the conventional fertilized ICON rotations mixed-maize (green), mixed-rice (blue) and paddy-rice (red). Dashed lines refer to the scenario simulations with 3.4 and 2.8 t C ha^{-1} yr^{-1} residue incorporation after harvest in the mixed–maize and mixed–rice rotation, respectively. Center: annual means of simulated ecosystem C fluxes for the different ICON rotations. Carbon fluxes represent soil organic carbon input via below- and aboveground plant litter and photosynthetic active aquatic biomass (PAB) as well as losses via emissions of CH_4 and CO_2. Right: balances of the respective simulated ecosystem C fluxes. (For interpretation of the references to colour in this figure legend, the reader is referred to the web version of this article.)

LTCCE0 treatment with suppressed growth of PAB, all other treatments still accumulate SOC in the year 2100, but with a decreasing annual SOC accumulation rate. For the control simulation, SOC stocks increase by 24 (LTCCE0) and 38% (LTCE360) in the time period 1963–2000, whereas in the time period 2063–2100 respective increases are 4 and 5%. The simulated equilibrium topsoil SOC stock in the LTCCE control amounts to approx. 30 t C ha^{-1} or to an equivalent SOC concentration of 2.2%.

Fig. 3 (right) illustrates the sensitivity of SOC stock dynamics in the LTFE0 and LTFE250 with regard to (a) shorter time periods of soil submergence, i.e., soil drainage two weeks before harvest and (b) increased decomposition of aboveground biomass by 50%. The two modifications lead to very similar reductions of simulated SOC stocks in both fertilizer regimes. For the reference year 2100, simulated SOC stocks in the LTFE0 and LTFE250 are always approx. 10% lower as compared to the respective default setting.

3.2.2. ICON experiment

In contrast to the LTCCE and LTFE, the ICON experiment was started only recently (2012). We only show predictive simulation results since spatial variability of carbon stocks still masks significant land management effects (Weller et al., 2016). Fig. 4 (left) illustrates the temporal development of topsoil SOC stocks and major carbon fluxes of the conventional fertilized mixed-maize, mixed-rice and paddy rice rotations until the year 2100. While the simulated topsoil SOC stock equilibrium of the paddy rice rotation essentially remains at the observed initial value, the model predicts substantial losses of 5.8 and 9.2 t C ha^{-1} (66 and 105 kg C ha^{-1} yr^{-1}) for the mixed-rice and mixed-maize rotations, respectively. Most SOC losses occur until 2050, i.e., 66 and 85%, respectively. Simulated carbon losses are the results of lower carbon input and, at the same time, increased respiratory carbon losses (Fig. 4). Average annual carbon inputs in the mixed-maize, mixed-rice and paddy rice rotation amount to 3.1, 3.9, 4.3 t C ha^{-1} yr^{-1}, respectively. The ratios of annual carbon input to carbon losses in the mixed-maize, mixed-rice and paddy rice rotation are −3.4, −1.5 and +0.2%, respectively.

For the evaluation of the required amount of carbon input in order to achieve stable SOC stocks in the mixed–maize and mixed–rice rotations, we performed scenario simulations with increased harvest residues. The simulation results suggest that the incorporation of approx. 3.4 and 2.8 t C ha^{-1} yr^{-1} harvest residues into the soil would lead to stable SOC stocks in the mixed–maize and mixed–rice rotation, respectively (Fig. 4, left).

3.3. CH_4 and N_2O emissions

Simulated and measured emissions of CH_4 and N_2O for the conventional fertilizer treatment of the ICON mixed-maize, mixed-rice and paddy rice rotation exhibit a strong seasonal pattern (see Fig. 5). The model simulates dynamics of CH_4 and N_2O emissions on daily time step with R^2 values in the range 0.58–0.71 and 0.01–0.27, respectively (Table 3). Model efficiencies for CH_4 emissions are in the range 0.56–0.59, while for N_2O only the mixed-maize rotation can be reproduced with a positive NSE value of 0.24 (Table 3).

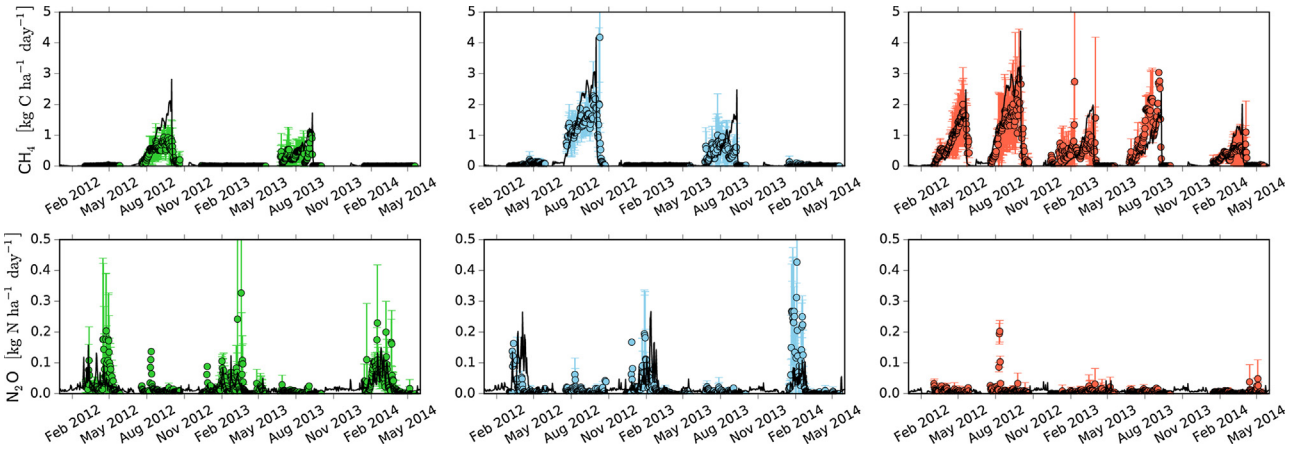

Fig. 5. Day-to-day comparisons of simulated and observed CH_4 and N_2O emissions for the conventional fertilized mixed-maize (green, left), mixed-rice (blue, center) and paddy rice rotations (red, right). Error bars represent the standard deviation of measured fluxes (n = 3). (For interpretation of the references to colour in this figure legend, the reader is referred to the web version of this article.)

Table 3
Model performance for day to day comparison of simulated and observed emissions of CH_4 and N_2O in the conventional fertilizer treatment of the mixed-maize, mixed-rice and paddy-rice rotation in the ICON experiment.

		R^2[a] [-]	NSE[b] [-]	RMSPE[c] [kg C/N ha^{-1} days^{-1}]
CH_4	Mixed-maize	0.71	0.59	0.29
	Mixed-rice	0.67	0.66	0.42
	Paddy-rice	0.58	0.56	0.53
N_2O	Mixed-maize	0.27	0.24	0.03
	Mixed-rice	0.07	−0.25	0.05
	Paddy-rice	0.01	−0.23	0.02

[a] Coefficient of Determination.
[b] Nash-Sutcliffe Efficiency.
[c] Root Mean Square Prediction Error.

Seasonal aggregated emissions (note that seasons refer to the time period of available measurements, i.e., no extrapolation) of CH_4 and N_2O of all different rotations and fertilizer treatments are simulated with R^2 values of 0.85 and 0.78 respectively (Fig. 6). Emissions of CH_4 are underestimated on average by 15%, mainly due to the underestimation of CH_4 fluxes for the unfertilized treatments. If the unfertilized treatments are excluded, an R^2 value of 0.92 is obtained, with seasonal aggregated fluxes being overestimated by 6% on average (data not shown).

Seasonal emissions of N_2O are underestimated by 14%. The highest observed seasonal emission is 7.3 kg N_2O-N ha^{-1} for the site-specific optimized fertilizer treatment of the mixed-maize rotation in the DS 2014 (simulated: 4.8 kg N_2O-N ha^{-1}, point 40 in Fig. 6), while maximum simulated emissions are 5.7 kg N_2O-N ha^{-1} for the site-specific optimized fertilizer treatment of the mixed-rice rotation in DS 2012 (observed: 5.2 kg N_2O-N ha^{-1}, point 23 in Fig. 7).

3.4. Full GHG balance

Fig. 7 contrasts simulated total GHG emissions (CO_2, CH_4 and N_2O expressed in CO_2-eq) for the mixed-maize, mixed-rice and paddy rice rotation studied within the ICON experiment. Our simulations cover a three-year simulation period and show highest cumulative total GHG emissions for the mixed-maize (22.3 t CO_2-eq. ha^{-1}) and mixed-rice rotation (22.1 t CO_2-eq. ha^{-1}). Cumulative total GHG emissions for the paddy rice rotation amount to 17.1 t CO_2-eq. ha^{-1}. For the mixed-maize rotation, CO_2 is the largest contributor to the GHG balance (43%) followed by emissions of N_2O (35%) and CH_4 (22%). In the mixed-rice rotation, CH_4 and N_2O contribute equally to total GHG emissions (38 and 37%) followed by CO_2 (25%). Total GHG emissions of the paddy rice rotation are dominated by CH_4 emissions (82%) with minor contributions of N_2O (14%) and CO_2 (4%). In contrast to the short-term balance, simulated cumulative total GHG emissions until the year 2100 show highest total GHG emissions for the paddy rice rotation (550 t CO_2-eq. ha^{-1}), followed by the mixed-rice rotation (492 t CO_2-eq. ha^{-1}) and lowest total GHG emissions (340 t CO_2-eq. ha^{-1}) were simulated for the mixed-maize rotation. Considering a longer time scale for all rotations, CH_4 is the dominant GHG (mixed-maize: 54%, mixed-rice: 57%, paddy rice: 80%). For the mixed-maize and mixed-rice rotation contribution of N_2O emissions (mixed-maize: 43%, mixed-rice: 40%) are slightly lower than CH_4 emissions, while for the paddy rice rotation N_2O emissions contribute on a much lower level to the total GHG balance (each by 10%). Influence of CO_2 on the total GHG balance was lowest (<10%) in all rotations, however, functioned as source for the mixed-maize and mixed-rice systems and sink in the paddy rice rotation.

4. Discussion

4.1. Above- and belowground biomass production

Crop growth influences emissions of the GHG CO_2, CH_4 and N_2O. Up to 50% of assimilated carbon can be transferred and released belowground (Kuzyakov and Domanski, 2000) where it might be sequestered as SOC (Rees et al., 2005) or serves as substrate for methanogenesis (Holzapfel-Pschorn et al., 1986) and denitrification (Butterbach-Bahl et al., 2013). Aboveground biomass (AGB) of rice in general is positively correlated with solar radiation (Dobermann et al., 2000; Evans and De Datta, 1979). In the Philippines, solar radiation and thus also AGB is higher in the dry season (DS) as compared to the wet season (WS) (Dobermann et al., 2000; Yang et al., 2008). LandscapeDNDC simulations reflect this

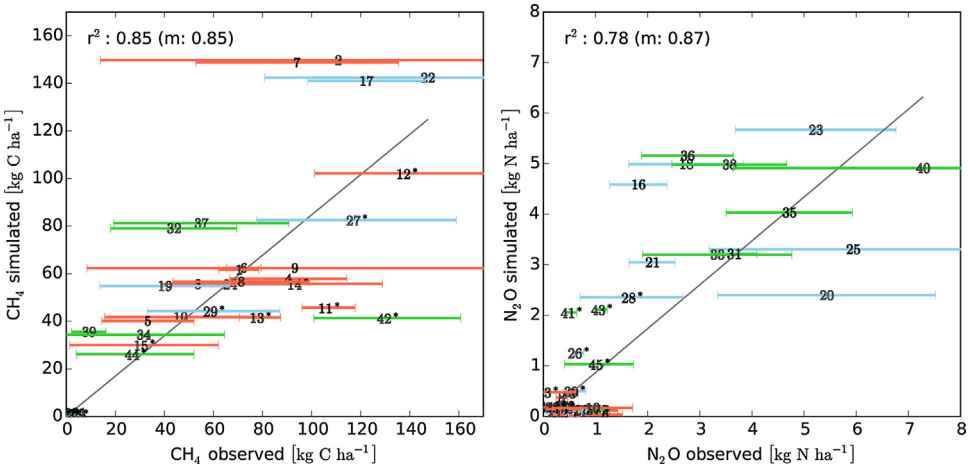

Fig. 6. Observed versus simulated seasonal emissions of CH_4 and N_2O for the mixed-maize (green), mixed-rice (blue) and paddy-rice (red) rotation system in the ICON experiment. Rotations without fertilizer application are marked (*). All seasonal emissions refer exclusively to the cropping time period where measurements are available (no extrapolation beyond times before first and after last measurement). The coefficients of determination (R^2) refer to the zero-regression line (y = mx). Seasons are given by: 1:rcd12, 2:rcw12, 3:rcd13, 4:rcw13, 5:rcw14, 6: rsd12, 7:rsw12, 8:rsd13, 9:rsw13, 10:rsd14, 11:rzd12, 12:rzw12, 13:rzd13, 14:rzw13, 15:rzd14, 16:acd12, 17:acw12, 18:acd13, 19:acw13, 20:acw14, 21:asd12, 22:asw12, 23:asd13, 24:asw13, 25:asd14, 26:azd12, 27:azw12, 28:azd13, 29:azw13, 30:azd14, 31:mcd12, 32:mcw12, 33:mcd13, 34:mcw13, 35:mcw14, 36:msd12, 37:msw12, 38:msd13, 39:msw13, 40:msd14, 41:mzd12, 42:mzw12, 43:mzd13, 44:mzw13, 45:mzd14. Code definition: rotation (r: paddy rice, a: aerobic rice, m: maize), fertilizer treatment (c: conventional, s: site specific optimized, z: no fertilizer), season (d: dry season, w: wet season) and year (12: 2012, 13: 2013, 14: 2014). (For interpretation of the references to colour in this figure legend, the reader is referred to the web version of this article.)

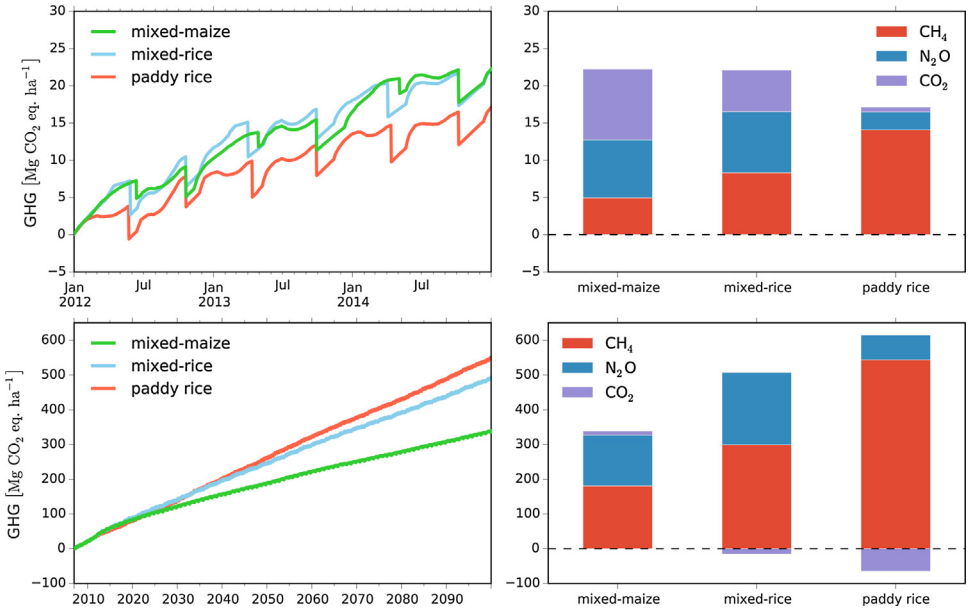

Fig. 7. Cumulative total GHG emissions of CO_2, CH_4 and N_2O for the mixed-maize, mixed-rice and paddy-rice rotation in the ICON experiment. Emissions are calculated for 3 (upper row) and 90 years (lower row) of unchanged management.

typical pattern of AGB, e.g., in the conventional fertilized paddy rice rotation in 2012. Observations for the unfertilized paddy rice rotation in 2012 show the opposite, i.e., higher AGB in the WS as compared to the DS. Such behavior is unexpected and may be attributed to problems with the field management, e.g., suboptimal irrigation in the DS. The overestimation of rice yields for the unfertilized mixed-maize rotation in the WS 2012 is likely due to a model underestimation of potential nutrient losses in the preceding DS.

During the two long-term continuous cropping experiments yields of all fertilizer treatments were reported to continuously decline from 1978 to 1990 (Cassman et al., 1995; Dobermann et al., 2000). From 1991 onwards, yields in the LTCCE are again comparable to the early phase of the experiment, which is mainly related to improved field management. The reason for the observed yield declines is not fully understood by the experimentalists. LandscapeDNDC failed to simulate yield declines as details on field management were missing. However, simulated average yields for LTCCE agreed with observed yields by ±10% providing confidence that simulated plant C input by aboveground residues and root litter are met accordingly. Bronson et al. (1998) estimate average annual carbon inputs via rice roots by 1.9 and 2.7 t C ha^{-1} yr^{-1} for the LTCCE0 and LTCCE360, respectively. Our simulations show similar values of 1.5 and 2.7 t C ha^{-1} yr^{-1} (Fig. 2).

4.2. SOC dynamics

SOC stocks are generally higher in paddy rice systems as compared to upland systems (Cheng et al., 2009; Huang et al., 2014; Pan et al., 2003, 2010; Sun et al., 2015; Wu, 2011). Higher SOC stocks result from higher biomass inputs (plant residues, organic fertilizer) and at the same time reduced decomposition in the absence of oxygen (Neue et al., 1997; Sahrawat, 2003). The growth of PAB is an additional important source of carbon that contributes to the accrual of SOC (Roger, 1996; Bronson et al., 1998; Pampolino et al., 2008). Gaydon et al. (2012) found that long-term SOC dynamics in paddy rice systems can only be reasonably explained by substantial carbon and nitrogen inputs via PAB. The simulation results of the LTCCE also suggest that SOC sequestration might be significantly underestimated without the consideration of PAB. The simulated annual carbon fixation of PAB corresponds to the mean value per cropping season of 0.5–0.6 t C ha^{-1} that has been reported for the Philippines (Saito and Watanabe, 1978). In addition to PAB, our uncertainty analysis shows that other factors, e.g., water management during the fallow period and land preparation also can strongly influence SOC development (Fig. 3). Maintaining fully water-saturated conditions during the fallow period significantly increases SOC stocks. Although this scenario is artificial, it demonstrates the general sensitivity of the magnitude of SOC stocks on the aeration status of the soil. Further emphasis on this is given by the LTFE for which annual carbon input is considerably larger as compared to the LTCCE. However, observed and simulated increases in SOC stocks in the LTFE are lower due to higher respiratory losses in view of an extended aerobic fallow period (double cropping) as compared to the LTCCE (triple copping). The reason for overestimating SOC stocks in the LTFE is likely linked to missing information on irrigation management. Our sensitivity analysis shows that assuming soil drainage two weeks before harvest results in significantly lower SOC stocks as in our standard runs for which drainage happened at harvest. Also an underestimation of rice straw decomposition might have contributed to the overestimation of increases in SOC stocks in the LTFE. There is evidence that root-derived biomass seems to contribute stronger to SOC formation than aboveground biomass (Lu et al., 2003; Kätterer et al., 2011). However, so far, $MeTr^x$ follows the approaches of other biogeochemical models, e.g., DECONIT or DNDC in using uniform decomposition constants for above- and belowground plant litter. Our second sensitivity analysis shows that increasing the decomposition constant for aboveground biomass only leads to reductions in the increase of SOC stocks with time, showing the need to consider the uncertain parameterization of litter decomposition dynamics while simulating changes in SOC stocks. Further factors, which might have affected long-term dynamics of SOC stocks relate to crop failure

due to, e.g., typhoons or crop diseases, which were not reported, but may have contributed to the communicated variation of soil C stocks in the LTFE.

The projective simulations of the mixed–maize, mixed–rice and paddy rice rotation of the ICON experiment predict substantial losses of SOC in rotations that replace paddy rice by an upland crop in the DS. In contrast, the SOC stock of the paddy rice rotation does not change over time and is well within usually observed topsoil SOC stocks of paddy rice systems. The simulation result of an equilibrium state of SOC is in accordance with our information that the fields at IRRI have been under double-cropped paddy rice cultivation for at least two decades. Simulated losses of SOC are more severe in the mixed–maize treatment than in the mixed–rice treatment, which is mostly attributed to the fact that all aboveground biomass from the maize plant is removed after harvest. For China, Pan et al. (2010) report approx. 60% higher SOC concentrations in paddy rice compared to upland crops. In a study on land management changes in the Philippines, Witt et al. (2000) report 11–12% higher carbon sequestration rates of paddy rice–paddy rice rotations compared to paddy rice–maize rotations. This is in good agreement with our simulations, as we show that the introduction of mixed systems might result in SOC stock decreases by 18% in 2100. However, in the Witt et al. (2000) study, SOC stocks remain essentially stable in the paddy rice–maize treatment, while they increase in the paddy rice–paddy rice treatment. The contrasting finding to our study (i.e., ICON data) can be explained by higher carbon inputs via remaining AGB. In the study of Witt et al. (2000), approx. 0.25–0.3 m rice stubble and 0.3–0.5 m maize stubble are left on the field after harvest (ICON rice: 0.1 m, ICON maize: 0.0 m), which is equal to approx. 1.0–2.0 and 0.9–1.0 t C ha^{-1}, respectively. In our scenario simulations approx. 3.4 and 2.8 t C ha^{-1} yr^{-1} of harvest residues are required to stabilize SOC stocks in the ICON mixed–maize and mixed–rice rotation, respectively. The higher amount of carbon input in our simulation can be explained by higher initial carbon stocks in the considered topsoil in the ICON fields (32 t C) as compared to the study of Witt et al. (2000) (19 t C). Despite the differences in, e.g., field management and soil properties, our simulation as well as the field study of Witt et al. (2000) agree that approx. 2–4 t C ha^{-1} yr^{-1} of harvest residues need to remain on the field to allow for stable SOC stocks in mixed lowland–upland cropping systems. In contrast to the study of Witt et al. (2000) and our simulations results, Linh et al. (2015) report increased SOC stocks after changing land management from triple-cropped paddy rice to double-cropped paddy rice plus one upland crop in the Mekong Delta region. The authors state that the increase in SOC stocks for rotations including one upland crop are related to a respective increase of the ploughing depth. This has resulted in an increase of SOC stocks in deeper soil layers while topsoil SOC stocks remained unaffected. However, a direct comparison possible to our study results is difficult as crop rotations and field management differ and information on the harvest index is missing. Nevertheless, the study of Linh et al. (2015) again demonstrates the sensitivity of SOC stocks to field management.

4.3. CH_4 and N_2O emissions

Continuously flooded rice cultivation emits significant amounts of CH_4 to the atmosphere, while emissions of N_2O are relatively low (Linquist et al., 2012; Weller et al., 2015a, 2016). Upland cropping systems, in contrast, show high N_2O emissions after fertilization but hardly any CH_4 emissions (Snyder et al., 2009; Weller et al., 2015a, 2016). As demonstrated in an earlier study (Kraus et al., 2015), the new LandscapeDNDC biogeochemical module $MeTr^x$ reasonably simulates the soil fluxes of CH_4 and N_2O under transient diversification of tropical lowland with upland systems. One main finding reported by Weller et al. (2016) is that emissions of CH_4 are significantly lower in the mixed–maize rotation as compared to the mixed–rice and paddy rice rotation. The model is able to reproduce this observation as lower carbon availability and larger oxidation of reduced iron in the mixed–maize rotation due to less irrigation and thus lower soil moisture (Weller et al., 2016) lead to reduced methanogenesis.

Across all rotations and fertilizer treatments, CH_4 emissions are underestimated by 15%. CH_4 emissions for unfertilized treatments were underestimated at most. In our model nitrogen fertilization promotes soil CH_4 oxidation as outlined in Bodelier and Laanbroek (2004). However, running the model with or without this N-factor for CH_4-oxidation has only a small effect on the underestimation of CH_4 emissions from unfertilized fields, i.e., from 58% (without) to 43% (with N-factor active) (data not shown). Thus, the finding of Weller et al. (2015a) who report that methane emissions in the ICON experiment were on average higher in the unfertilized compared to the fertilized crop rotations could not be reproduced. Numerous studies report both increased as well as decreased emissions of CH_4 under low nitrogen availability (Banger et al., 2012). Increased emissions are related to low methanotrophic activity under nitrogen deficiency (Bodelier and Laanbroek, 2004), while decreased emissions are related to lower biomass production which results in a reduced availability of methanogenic substrate (Huang et al., 1998). The latter point is reflected in the ICON experiment by comparing the mixed–rice to the mixed–maize rotation. Observed emissions of CH_4 for, e.g., the WS 2012 are considerably lower in the fertilized mixed–maize rotation (no residues left on the field) than in the fertilized mixed–rice rotation. In contrast, observed CH_4 emissions in the unfertilized treatment are essentially equal in both rotations. Apart from the unfertilized treatments, the model reflects well ($R^2 = 0.85$) observed differences in seasonal CH_4 emissions, with model results being well within the uncertainty range of measurements.

Predictive capability of LandscapeDNDC for the simulation of rice paddy systems in this study is generally lower for N_2O emissions than for CH_4 emissions. Especially day-to-day comparisons show low R^2 and NSE values, which was also the case in our earlier study (Kraus et al., 2015). This is mainly related to the more dynamic temporal emission patterns (e.g., lag effects, step-wise processing of nitrogen) and higher spatial variability of measured soil N_2O fluxes, both factors being represented in the large uncertainties of the field observations (Fig. 6). Seasonal emissions are significantly better represented ($R^2 = 0.78$) with an overall underestimation of 14%, but particularly in the DS and WS 2014 in the mixed–rice rotation (point 20 and 25 in Fig. 6). Weller et al. (2016) discuss that the high variations of observed N_2O emissions in the aerobic rice fields of the ICON experiment can be mainly explained by repeated drying/rewetting cycles in the upper soil layers.

4.4. Full GHG balance

The development of mitigation strategies that consider trade-offs between the reductions of individual GHG are based on metrics that allow the comparison of GHG against each other. The global warming potential (GWP) is by far the most frequently used metric, although, there is an ongoing debate whether it is also the most suitable one for predictions over longer time periods (Shine, 2009; Smith and Wigley, 2000). Simulated total GHG emissions in the ICON experiment three years after land management change are higher for the mixed lowland–upland rotation systems compared to the lowland paddy rice rotation. This is in contrast to Weller et al. (2016) who report that the paddy rice system exhibits the largest GHG emissions. The discrepancy between both studies is predominantly caused by the simulated larger SOC losses

in the first years after land management change. For the moment, the high spatial variability of observed SOC stocks prevents a quantitative comparison. However, since carbon stock simulations with LandscapeDNDC showed good agreement with observed SOC stock changes of the LTCCE and LTFE, we are confident that a future re-evaluation of stock changes 10 years after land management change will allow a better comparison. In contrast to the short-term GHG balances, long-term total GHG fluxes are highest in the lowland paddy rice system and dominated by CH_4 emissions. We do not discuss the absolute values due to the shortcomings of cumulative GWP on longer time scales (Frolking et al., 2004), however, the results qualitatively demonstrate that the radiative forcing of CH_4 emissions from paddy rice fields dominate over N_2O emissions from upland crops as has been also stated by Linquist et al. (2012) and Weller et al. (2016). In contrast to the short-term GHG balance, the importance of SOC stocks changes for the total GHG balance decreases over longer periods. This result is logical due to the establishment of new equilibriums of SOC stocks as triggered by carbon in- and output fluxes, while emissions of CH_4 from paddy rice fields and N_2O from upland cropping systems persist and cannot be balanced by respective uptake rates. However, we stress that apart from its radiative forcing lower equilibriums of SOC stocks may cause, e.g., lower soil fertility and thus will negatively feedback on the yield of respective cropping systems, which might be compensated by higher nitrogen fertilization with the risk of enhancing N_2O emissions.

5. Conclusion

In this study we evaluate LandscapeDNDC for its predicting capability of full GHG balances from differently managed tropical lowland, and lowland-upland rice based cropping systems. In agreement with field measurements our simulations show significant effects of field management on soil carbon stocks and N_2O and CH_4 emissions. We also show that short-term GHG balances (3 years) might significantly deviate from long-term GHG balances (>20–50 years), since the influence of changes in soil carbon stocks on the GHG balance diminishes with time, while CH_4 emissions during the paddy rice season (in all investigated treatments at least the wet season) gain in importance. These results further stress the importance of long-term (>10 years) field measurements, since only such measurements finally provide proof for model simulations. In addition, based on the long-term observations of SOC stock changes for different paddy rice cropping systems at IRRI as well as comparison to observations from mixed lowland–upland cropping systems, we also demonstrate that LandscapeDNDC is capable to reasonable simulate changes in soil C and N cycling and associated biosphere-atmosphere exchange for rice dominated agricultural systems in the tropics and subtropics. This leads us to believe that LandscapeDNDC can serve as valuable tool for investigating impacts of global environmental changes on C and N stocks and associated GHG budgets.

Acknowledgements

We thank the German Research Foundation (DFG) for its generous funding (FOR 1701, “Introducing Non-Flooded Crops in Rice-Dominated Landscapes: Impacts on Carbon, Nitrogen and Water Cycles (ICON)”, BU1173/13-1 and KI1413). KBB and RW received additional financial support via the Climate Change, Agricultural and Food Security Program (CCAFS) of CGIAR Institutes.

References

Aulakh, M.S., Wassmann, R., Bueno, C., Rennenberg, H., 2001. Impact of root exudates of different cultivars and plant development stages of rice (*Oryza sativa* L.) on methane production in a paddy soil. Plant Soil 230, 77–86.
Babu, Y.J., Li, C., Frolking, S., Nayak, D.R., Adhya, T.K., 2006. Field validation of DNDC model for methane and nitrous oxide emissions from rice-based production systems of India. Nutr. Cycl. Agroecosyst. 74, 157–174. doi:http://dx.doi.org/10.1007/s10705-005-6111-5.
Banger, K., Tian, H., Lu, C., 2012. Do nitrogen fertilizers stimulate or inhibit methane emissions from rice fields? Global Change Biol. 18, 3259–3267. doi:http://dx.doi.org/10.1111/j.1365-2486.2012.02762.x.
Bodelier, P.L.E., Laanbroek, H.J., 2004. Nitrogen as a regulatory factor of methane oxidation in soils and sediments. FEMS Microbiol. Ecol. 47, 265–277.
Boucher, O., Friedlingstein, P., Collins, B., Shine, K.P., 2009. The indirect global warming potential and global temperature change potential due to methane oxidation. Environ. Res. Lett. 4, 044007. doi:http://dx.doi.org/10.1088/1748-9326/4/4/044007.
Bouman, B.A.M., Tuong, T.P., 2001. Field water management to save water and increase its productivity in irrigated lowland rice. Agric Water Manage. 49, 11–30.
Bouman, B.A.M., Humphreys, E., Tuong, T.P., Barker, R., 2007. Rice and water. Adv. Agron. 92, 187–237.
Bronson, K.F., Cassman, K.G., Wassmann, R., Olk, D.C., van Noordwijk, M., Garrity, D.P., 1998. Soil carbon dynamics in different cropping systems in principal ecoregions of asia. In: Lal, R., Kimble, J., Follett, R.F., Stewart, B.A. (Eds.), Management of Carbon Sequestration in Soil. CRC Press, Boca Raton, FL, pp. 35–57.
Butterbach-Bahl, K., Baggs, E.M., Dannenmann, M., Kiese, R., Zechmeister-Boltenstern, S., 2013. Nitrous oxide emissions from soils: how well do we understand the processes and their controls? Philos. Trans. R. Soc. Lond. B Biol. Sci. 368, 20130122. doi:http://dx.doi.org/10.1098/rstb.2013.0122.
Cassman, K.G., De Datta, D.C., Olk, D.C., Alcantara, J., Samson, J., Descalsota, J., Dizon, M., 1995. Yield decline and the nitrogen economy of long-term experiments on continuous, irrigated rice systems in the tropics. In: Lal, R., Stewart, B.A. (Eds.), Soil Management: Experimental Basis for Sustainability and Environmental Quality. CRC Press, Boca Raton, FL, pp. 181–222.
Cheng, Y.Q., Yang, L.Z., Cao, Z.H., Yin, S., 2009. Chronosequential changes of selected pedogenic properties in paddy soils as compared with non-paddy soils. Geoderma 151, 31–41.
Cheng, K., Ogle, S.M., Parton, W.J., Pan, G., 2014. Simulating greenhouse gas mitigation potentials for Chinese Croplands using the DAYCENT ecosystem model. Global Change Biol. 20, 948–962. doi:http://dx.doi.org/10.1111/gcb.12368.
Chirinda, N., Kracher, D., Lægdsmand, M., Porter, J.R., Olesen, J.E., Petersen, B.M., Doltra, J., Kiese, R., Butterbach-Bahl, K., 2011. Simulating soil N_2O emissions and heterotrophic CO_2 respiration in arable systems using FASSET and MoBiLE-DNDC. Plant Soil 343, 139–160.
Ciais, P., Sabine, C., Bala, G., Bopp, L., Brovkin, V., Canadell, J., Chhabra, A., DeFries, R., Galloway, J., Heimann, M., Jones, C., Le Quéré, C., Myneni, R.B., Piao, S., Thornton, P., 2013. Carbon and other biogeochemical cycles. In: Stocker, T.F., Qin, D., Plattner, G.-K., Tignor, M., Allen, S.K., Boschung, J., Nauels, A., Xia, Y., Bex, V., Midgley, P.M. (Eds.), Climate Change 2013: The Physical Science Basis. Contribution of Working Group I to the Fifth Assessment Report of the Intergovernmental Panel on Climate Change. Cambridge University Press Cambridge, United Kingdom and New York, NY, USA.
Denman, K.L., Brasseur, G., Chidthaisong, A., Ciais, P., Cox, P.M., Dickinson, R.E., Hauglustaine, D., Heinze, C., Holland, E., Jacob, D., Lohmann, U., Ramachandran, S., da Silva Dias, P.L., Wofsy, S.C., Zhang, X., 2007. Couplings between changes in the climate system and biogeochemistry. In: Solomon, S., Qin, D., Manning, M., Chen, Z., Marquis, M., Averyt, K.B., Tignor, M., Miller, H.L. (Eds.), Climate Change 2007: The Physical Science Basis. Contribution of Working Group I to the Fourth Assessment Report of the Intergovernmental Panel on Climate Change. Cambridge University Press, Cambridge.
Devendra, C., Thomas, D., 2002. Smallholder farming systems in Asia. Agric. Syst. 71, 17–25.
Dirnböck, T., Kobler, J., Kraus, D., Grote, R., Kiese, R., 2016. Impacts of climate change on nitrate leaching in a managed forest in the Northern Limestone Alps. Aust. J. Environ. Manage. 165, 243–252. doi:http://dx.doi.org/10.1016/j.jenvman.2015.09.039.
Dobermann, A., Dawe, D., Roetter, R.P., Cassman, K.G., 2000. Reversal of Rice Yield Decline in a Long-Term Continuous Cropping Experiment. Agronomy & Horticulture – Faculty Publications Paper 91.
Don, A., Schumacher, J., Freibauer, A., 2011. Impact of tropical land-use change on soil organic carbon stocks—a meta-analysis. Global Change Biol. 17, 1658–1670. doi:http://dx.doi.org/10.1111/j.1365-2486.2010.02336.x.
Evans, L.T., De Datta, S.K., 1979. The relation between irradiance and grain yield of irrigated rice in the tropics as influenced by cultivar, nitrogen fertilizer application, and month of planting. Field Crops Res. 2, 1–17.
Frolking, S., Li, C., Braswell, R., Fuglestvedt, J., 2004. Short- and long-term greenhouse gas and radiative forcing impacts of changing water management in Asian rice paddies. Global Change Biol. 10, 1180–1196. doi:http://dx.doi.org/10.1111/j.1365-2486.2004.00798.x.
Gaydon, D.S., Probert, M.E., Buresh, R.J., Meinke, H., 2012. Modelling the role of algae in rice crop nutrition and soil organic carbon maintenance. Europ. J. Agron. 39 (2012), 35–43. doi:http://dx.doi.org/10.1016/j.eja.2012.01.004.

Grote, R., Lehmann, E., Brümmer, C., Brüggemann, N., Szarzynski, L., Kunstmann, H., 2009. Modelling and observation of biosphere–atmosphere interactions in natural savannah in Burkina Faso, West Africa. Phys. Chem. Earth 34, 251–260. doi:http://dx.doi.org/10.1016/j.pce.2008.05.003.

Häfele, S.M., Banayo, N.P.M., Amarante, S.T., Siopongco, J.D.L.C., Mabesa, R., 2013. Characteristics and management options for rice-maize systems in the Philippines. Field Crops Res. 144, 52–61.

Haas, E., Klatt, S., Fröhlich, A., Kraft, P., Werner, C., Kiese, R., Grote, R., Breuer, L., Butterbach-Bahl, K., 2013. LandscapeDNDC: a process model for simulation of biosphere–atmosphere–hydrosphere exchange processes at site and regional scale. Landscape Ecol. 28, 615–636. doi:http://dx.doi.org/10.1007/s10980-012-9772-x.

Herzog, T., 2009. World Greenhouse Gas Emissions in 2005. WRI Working Paper in 2005World Resources Institute. . (accessed August 2015) http://www.wri.org/publication/navigating-the-numbers.

Holzapfel-Pschorn, A., Conrad, R., Seiler, W., 1986. Effects of vegetation on the emission of methane from submerged paddy soil. Plant Soil 92, 223–233.

Huang, Y., Sass, R.L., Fisher Jr., F.M., 1998. A semi-empirical model of methane emission from flooded rice paddy soils. Global Change Biol. 4, 247–268. doi:http://dx.doi.org/10.1046/j.1365-2486.1998.00129.x.

Huang, S., Sun, Y., Zhang, W., 2012. Changes in soil organic carbon stocks as affected by cropping systems and cropping duration in China's paddy fields: a meta-analysis. Clim. Change 112, 847–858. doi:http://dx.doi.org/10.1007/s10584-011-0255-x.

Huang, S., Pan, X., Guo, J., Qian, C., Zhang, W., 2014. Differences in soil organic carbon stocks and fraction distributions between rice paddies and upland cropping systems in China. J. Soils Sediments 14, 89–98. doi:http://dx.doi.org/10.1007/s11368-013-0789-9.

Johnston, A.E., Poulton, P.R., Coleman, K., 2009. Soil organic matter: its importance in sustainable agriculture and carbon dioxide fluxes. Adv. Agron. 101, 1–57.

Kätterer, T., Bolinder, M.A., Andrén, O., Kirchmann, H., Menichetti, L., 2011. Roots contribute more to refractory soil organic matter than above-ground crop residues, as revealed by a long-term field experiment. Agric. Ecosyst. Environ. 141, 184–192. doi:http://dx.doi.org/10.1016/j.agee.2011.02.029.

Kögel-Knabner, I., Amelung, W., Cao, Z., Fiedler, S., Frenzel, P., Jahn, R., Kalbitz, K., Kölbl, A., Schloter, M., 2010. Biogeochemistry of paddy soils. Geoderma 157, 1–14. doi:http://dx.doi.org/10.1016/j.geoderma.2010.03.009.

Kim, Y., Berger, S., Kettering, J., Tenhunen, J., Haas, E., Kiese, R., 2014. Simulation of N_2O emissions and nitrate leaching from plastic mulch radish cultivation with LandscapeDNDC. Ecol. Res. 29, 441–454. doi:http://dx.doi.org/10.1007/s11284-014-1136-3.

Kim, Y., Seo, Y., Kraus, D., Klatt, S., Haas, E., Tenhunen, J., Kiese, R., 2015. Estimation and mitigation of N_2O emission and nitrate leaching from intensive crop cultivation in the Haean catchment, South Korea. Sci. Total Environ. 529, 40–53. doi:http://dx.doi.org/10.1016/j.scitotenv.2015.04.098.

Kraus, D., Weller, S., Klatt, S., Haas, E., Wassmann, R., Kiese, R., Butterbach-Bahl, K., 2015. A new LandscapeDNDC biogeochemical module to predict CH_4 and N_2O emissions from lowland rice and upland cropping systems. Plant Soil 386, 125–149. doi:http://dx.doi.org/10.1007/s11104-014-2255-x.

Kuzyakov, Y., Domanski, G., 2000. Carbon input by plants into the soil. Review. J. Plant Nutr. Soil Sci. 163, 421–431.

Li, C., Aber, J., Stange, F., Butterbach-Bahl, K., Papen, H., 2000. A process-oriented model of N_2O and NO emissions from forest soils: 1. Model development. J. Geophys. Res. Atmos. 105, 4369–4384. doi:http://dx.doi.org/10.1029/1999JD900949.

Li, C., Frolking, S.E., Butterbach-Bahl, K., 2005. Carbon sequestration in arable soils is likely to increase nitrous oxide emissions, offsetting reductions in climate radiative forcing. Clim. Change 72, 321–338. doi:http://dx.doi.org/10.1007/s10584-005-6791-5.

Linquist, B., van Groenigen, K.J., Adviento-Borbe, M.A., Pittelkow, C., van Kessel, C., 2012. An agronomic assessment of greenhouse gas emissions from major cereal crops. Global Change Biol. 18, 194–209.

Linh, T.B., Sleutel, S., Elsacker, S.V., Guong, V.T., Khoa, L.V., Cornelis, W.M., 2015. Inclusion of upland crops in rice-based rotations affects chemical properties of clay soil. Soil Use Manag. 31, 313–320. doi:http://dx.doi.org/10.1111/sum.12174.

Lu, Y., Watanabe, A., Kimura, M., 2003. Carbon dynamics of rhizodeposits, root- and shoot-residues in a rice soil. Soil Biol. Biochem. 35, 1223–1230. doi:http://dx.doi.org/10.1016/S0038-0717(03)00184-6.

Molina-Herrera, S., Grote, R., Santabárbara-Ruiz, I., Kraus, D., Klatt, S., Haas, E., Kiese, R., Butterbach-Bahl, K., 2015. Simulation of CO_2 fluxes in european forest ecosystems with the coupled soil-vegetation process model LandscapeDNDC. Forests 6, 1779–1809. doi:http://dx.doi.org/10.3390/f6061779.

Molina-Herrera, S., Haas, E., Klatt, S., Kraus, D., Augustin, J., Magliulo, V., Tallec, T., Ceschia, E., Ammann, C., Loubet, B., Skiba, U., Jones, S., Brümmer, C., Butterbach-Bahl, K., Kiese, R., 2016. A modelling study on mitigation of N_2O emissions and NO_3 leaching at different agricultural sites across Europe using LandscapeDNDC. Sci. Total Environ. 553, 128–140.

Myhre, G., Shindell, D., Bréon, F.M., Collins, W., Fuglestvedt, J., Huang, J., Koch, D., Lamarque, J.F., Lee, D., Mendoza, B., Nakajima, T., Robock, A., Stephens, G., Takemura, T., Zhang, H., 2013. Anthropogenic and natural radiative forcing. In: Stocker, T.F., Qin, D., Plattner, G.-K., Tignor, M., Allen, S.K., Boschung, J., Nauels, A., Xia, Y., Bex, V., Midgley, P.M. (Eds.), Climate Change 2013: The Physical Science Basis. Contribution of Working Group I to the Fifth Assessment Report of the Intergovernmental Panel on Climate Change. Cambridge University Press Cambridge, United Kingdom and New York, NY, USA.

Neue, H.U., Gaunt, J.L., Wang, Z.P., Becker-Heidmann, P., Quijano, C., 1997. Carbon in tropical wetlands. Geoderma 79, 163–185.

Olk, D.C., Cassman, K.G., Randall, E.W., Kinchesh, P., Sanger, L.J., Anderson, J.M., 1996. Changes in chemical properties of organic matter with intensified rice cropping in tropical lowland soil. Eur. J. Soil Sci. 47, 293–303.

Pampolino, M.F., Laureles, E.V., Gines, H.C., Buresh, R.J., 2008. Soil carbon and nitrogen changes in long-term continuous lowland rice cropping. Soil Sci. Soc. Am. J. 72, 798. doi:http://dx.doi.org/10.2136/sssaj2006.0334.

Pan, G.X., Li, L.Q., Wu, L.S., Zhang, X.H., 2003. Storage and sequestration potential of topsoil organic carbon in China's paddy soils. Global Change Biol. 10, 79–92.

Pan, G., Xu, X., Smith, P., Pan, W., Lal, R., 2010. An increase in topsoil SOC stock of China's croplands between 1985 and 2006 revealed by soil monitoring. Agric. Ecosyst. Environ. 136, 133–138. doi:http://dx.doi.org/10.1016/j.agee.2009.12.011.

Roger, P.A., 1996. Biology and Management of the Floodwater Ecosystem in Rice Fields. IRRI, Los Baños.

Rees, R.M., Bingham, I.J., Baddeley, J.A., Watson, C.A., 2005. The role of plants and land management in sequestering soil carbon in temperate arable and grassland ecosystems. Geoderma. Mech. Regul. Org. Matter Stabilisation Soils 128, 130–154. doi:http://dx.doi.org/10.1016/j.geoderma.2004.12.020.

Sahrawat, K.L., 2003. Organic matter accumulation in submerged soils. Advances in Agronomy, vol. 81. Elsevier, pp. 169–201. doi:http://dx.doi.org/10.1016/S0065-2113(03)81004-0.

Saito, M., Watanabe, I., 1978. Organic matter production in rice field flood water. Soil Sci. Plant Nutr. 24, 427–440. doi:http://dx.doi.org/10.1080/00380768.1978.10433121.

Shang, Q., Yang, X., Gao, C., Wu, P., Liu, J., Xu, Y., Shen, Q., Zou, J., Guo, S., 2011. Net annual global warming potential and greenhouse gas intensity in Chinese double rice-cropping systems: a 3-year field measurement in long-term fertilizer experiments. Global Change Biol. 17, 2196–2210. doi:http://dx.doi.org/10.1111/j.1365-2486.2010.02374.x.

Shine, K.P., 2009. The global warming potential—the need for an interdisciplinary retrial. Clim. Change 96, 467–472. doi:http://dx.doi.org/10.1007/s10584-009-9647-6.

Smith, S.J., Wigley, T.M.L., 2000. Global warming potentials: 1: climatic implications of emission reductions. Clim. Change 44, 445–457.

Snyder, C.S., Bruulsema, T.W., Jensen, T.L., Fixen, P.E., 2009. Review of greenhouse gas emissions from crop production systems and fertilizer management effects. Reactive nitrogen in agroecosystems: integration with greenhouse gas interactions. Agric. Ecosyst. Environ. 133, 247–266.

Sun, Y., Huang, S., Yu, X., Zhang, W., 2015. Differences in fertilization impacts on organic carbon content and stability in a paddy and an upland soil in subtropical China. Plant Soil doi:http://dx.doi.org/10.1007/s11104-015-2611-5.

Timsina, J., Jat, M., Majumdar, K., 2010. Rice-maize systems of South Asia: current status: future prospects and research priorities for nutrient management. Plant Soil 335, 65–82.

Timsina, J., Buresh, R.J., Dobermann, A., Dixon, J., 2011. Rice-maize Systems in Asia: Current Situation and Potential. International Rice Research Institute and International Maize and Wheat Improvement Center, Los Baños.

Wassmann, R., Neue, H.U., Ladha, J.K., Aulakh, M.S., 2004. Mitigating greenhouse gas emissions from rice-wheat cropping systems in asia. Environ. Dev. Sustainability 6, 65–90.

Weller, S., Kraus, D., Ayag, K.R.P., Wassmann, R., Alberto, M.C.R., Butterbach-Bahl, K., Kiese, R., 2015a. Methane and nitrous oxide emissions from rice and maize production in diversified rice cropping systems. Nutr. Cycl. Agroecosyst. 101, 37–53. doi:http://dx.doi.org/10.1007/s10705-014-9658-1.

Weller, S., Kraus, D., Butterbach-Bahl, K., Wassmann, R., Tirol-Padre, A., Kiese, R., 2015b. Diurnal patterns of methane emissions from paddy rice fields in the Philippines. J. Plant Nutr. Soil Sci. 178, 755–767. doi:http://dx.doi.org/10.1002/jpln.201500092.

Weller, S., Janz, B., Jörg, L., Kraus, D., Racela, H.S., Wassmann, R., Butterbach-Bahl, K., Kiese, R., 2016. Greenhouse gas emissions and global warming potential of traditional and diversified tropical rice rotation systems. Global Change Biol. 22, 432–448. doi:http://dx.doi.org/10.1111/gcb.13099.

Witt, C., Cassman, K.G., Olk, D.C., Biker, U., Liboon, S.P., Samson, M.I., Ottow, J.C.G., 2000. Crop rotation and residue management effects on carbon sequestration, nitrogen cycling and productivity of irrigated rice systems. Plant Soil 225, 263–278. doi:http://dx.doi.org/10.1023/A:1026594118145.

Wolf, B., Kiese, R., Chen, W., Grote, R., Zheng, X., Butterbach-Bahl, K., 2012. Modeling N_2O emissions from steppe in Inner Mongolia China, with consideration of spring thaw and grazing intensity. Plant Soil 350, 297–310. doi:http://dx.doi.org/10.1007/s11104-011-0908-6.

Wu, J., 2011. Carbon accumulation in paddy ecosystems in subtropical China: evidence from landscape studies. Eur. J. Soil Sci. 62, 29–34. doi:http://dx.doi.org/10.1111/j.1365-2389.2010.01325.x.

Yadav, R.L., Yadav, D.S., Singh, R.M., Kumar, A., 1998. Long term effects of inorganic fertilizer inputs on crop productivity in a rice-wheat cropping system. Nutr. Cycl. Agroecosyst. 51, 193–200.

Yao, H., Conrad, R., Wassmann, R., Neue, H.U., 1999. Effect of soil characteristics on sequential reduction and methane production in sixteen rice paddy soils from China, the Philippines, and Italy. Biogeochemistry 47, 269–295. doi:http://dx.doi.org/10.1007/BF00992910.

Yang, W., Peng, S., Laza, R.C., Visperas, R.M., Dionisio-Sese, M.L., 2008. Yield gap analysis between dry and wet season rice crop growth under high-yielding management conditions. Agron. J. 100, 1390–1395.